

# **Perturbation calculus for eikonal application to analysis of the deflectional signal in photothermal measurements**

ROMAN J. BUKOWSKI, DOROTA KORTE

Institute of Physics, Silesian University of Technology, ul. Krzywoustego 2, 44–100 Gliwice, Poland.

Using complex geometrical optics methods the influence of a one dimensional plane thermal wave on probing Gaussian beam phase was analysed. Detection of the probing beam parameters by quadrant photodiode was investigated. The dependence of the photodiode current signal on probing beam diameter, its waist, sample position, angular modulation frequency, the height of the beam over the sample and the focal length of the lens at the input of experimental setup was studied.

## **1. Introduction**

Nowadays, investigation into the solid state thermal properties is of great importance, especially for different nonhomogeneous layered systems. Some of the most essential are such photothermal methods which consider the differences between thermal properties of different parts of the layered system. Temperature changes in such a system are measured directly or indirectly, which finally, allows us to conclude about its structure.

One of the indirect methods for measuring changes of sample surface temperature is a photodeflectional method. In this method, the periodically heated sample makes the surrounding gas temperature change, resulting in changes of the gas refraction index. The latter changes are detected by probing light beam with known light intensity distribution passing through the heated gas layer. The gas refraction index changes cause the phase change in the probing beam.

At present, two theoretical methods for description of these phenomena are used [1], [2]. The first one is the ray method. It is based on the small shift of light beam (deflection) in nonhomogeneous media. There is also a generalization of that method for wide probing beams [3], [4]. The second method is the wave one [2]. In this work, a wave equation was solved for the probing beam propagation but only its phase change was taken into consideration.

A complete (with arbitrary accuracy) description of light beam propagation in optically nonhomogeneous medium can be achieved by geometrical optics method, for example by means of Debye's expansion [5]–[7]. A proper analysis using complex geometrical optics methods and taking into account the phase change of probing light beam, caused by thermal waves, is presented in [7], [8].



The first equation is called eikonal one and the others are transport equations of the 1st, 2nd order, and so on.

Boundary condition for Helmholtz's equation can be found by defining the electric field  $u^0(\xi, \eta)$  on a surface  $Q$ , the equation of which can be written in a parametric form

$$\mathbf{r} = \mathbf{r}_0(\xi, \eta) \tag{6}$$

where  $\xi, \eta$  – curvilinear coordinates on surface  $Q$ .

In the case of geometrical optics, the field  $u^0(\xi, \eta)$  should also be presented in the form of Debye's expansion

$$u^0(\xi, \eta) = \sum_{m=0}^{\infty} \frac{A_m^0(\xi, \eta)}{(ik_0)^m} \exp(ik_0\psi^0(\xi, \eta)). \tag{7}$$

Therefore

$$\psi|_Q = \psi^0(\xi, \eta), \quad A_m|_Q = A_m^0(\xi, \eta). \tag{8}$$

### 3. Gaussian beam in an optically homogenous medium

From [6] it follows that the electric field distribution in Gaussian beam with radius  $a$  and wavelength  $\lambda$  (wave number  $k = 2\pi/\lambda$ ) which propagates in homogenous medium with refraction index  $n_0$  can be written as

$$u(x, y, z) = A_0(\mathbf{r}) \exp(ik\psi_0(\mathbf{r})) \tag{9}$$

where

$$A_0(\mathbf{r}) = E_0 \left( 1 + \frac{i(z-L)}{z_R} \right)^{-1},$$

$$\psi_0(\mathbf{r}) = (z-L)n_0 + in_0 \frac{x^2 + y^2}{2z_R} \left( 1 + \frac{i(z-L)}{z_R} \right)^{-1}. \tag{10}$$

The beam enters the system in the plane  $z = 0$  and propagates in the plus direction of the  $OZ$  axis, and its waist is placed in the plane  $z = L$ .  $E_0$  is the electric field intensity in the middle of the waist. The parameter  $z_R = ka^2n_0$  is called Rayleigh's length, the quantity  $\psi_0$  – wave eikonal, and  $A_0$  – its amplitude (of the zero order). The beam ray coordinates  $\mathbf{r}(\tau) = [x(\tau), y(\tau), z(\tau)]$  are defined by equations:

$$x(\tau) = \xi + \frac{i\xi}{z_R} n_0 \left( 1 - \frac{iL}{z_R} \right)^{-1} \tau,$$

$$y(\tau) = \eta + \frac{i\eta}{z_R} n_0 \left( 1 - \frac{iL}{z_R} \right)^{-1} \tau,$$

$$z(\tau) = n_0 \tau \sqrt{1 + \frac{(\xi^2 + \eta^2)}{z_R^2} \left(1 - \frac{iL}{z_R}\right)^{-2}} \quad (11)$$

where  $\xi, \eta$  are the ray start point coordinates from the plane  $z = 0$  ( $XY$ ), and  $\tau$  is the running coordinate (in general case the complex one) along the ray.

For a given observation point  $\mathbf{r}_D = [x_D, y_D, z_D]$  (e.g., a point in the detection plane) we need to find all rays coming into that point, i.e., the solution of the set of Eq. (11), relatively to “rays” variable  $[\xi, \eta, \tau]$ , needs to be found (the so-called geometrical optics reversal problem). After linearization we have

$$\begin{aligned} \tau_D &\equiv \frac{z_D}{n_0} \left[ 1 - \frac{(\xi^2 + \eta^2)}{2z_R^2} \left(1 - \frac{iL}{z_R}\right)^{-2} \right] \equiv \frac{z_D}{n_0}, \\ \xi_D &\equiv x_D \left[ 1 + \frac{iz_D}{z_R} \left(1 - \frac{iL}{z_R}\right)^{-1} \right]^{-1}, \\ \eta_D &\equiv y_D \left[ 1 + \frac{iz_D}{z_R} \left(1 - \frac{iL}{z_R}\right)^{-1} \right]^{-1}. \end{aligned} \quad (12)$$

It follows from this solution that for such a simplification we have a particularly simple situation, i.e., only one ray comes to all observation points. Equations (12) define exactly the start point of the ray  $(\xi, \eta)$  when its observation point  $(x_D, y_D, z_D)$  is known.

#### 4. Gaussian beam in a thermally disturbed medium

Let us consider a standard experimental setup scheme for the solid state photothermal investigation with photodeflectional detection (Fig. 1). Modulated light beam incident on the sample gives it periodically specified energy flux. As a result the sample and surrounding gas (e.g., air) are heated and in stationary state we deal with temperature changing periodically in time and space, so-called thermal waves. These thermal waves cause changes in the gas refraction index, which brings about of the probing beam parameters modification. In the first approximation we can assume that

$$n(T) = n_0 + \left. \frac{dn}{dT} \right|_{T_0} (T - T_0) = n_0 + n_0 s_T (T - T_0), \quad T_0 = \text{const}(\mathbf{r}) \quad (13)$$

where  $n_0$  – gas refraction index in temperature  $T_0$ ,  $s_T$  – refraction index thermal sensitivity, and

$$s_T = \frac{1}{n_0} \frac{dn(T_0)}{dT}.$$

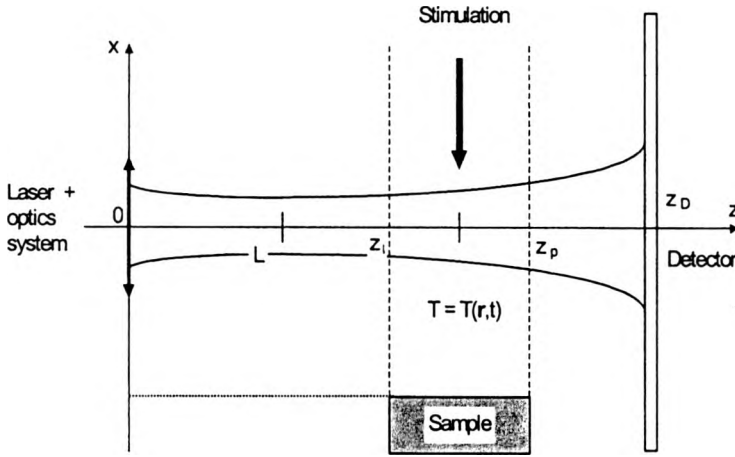


Fig. 1. Experimental setup scheme for solid state investigation by photothermal method with photodeflectional detection. The gas heated region have the width  $\Delta z = z_p - z_i$  and its left edge distance from the setup beginning (light beam “input”) is equal  $z_i$ . We assume that the heated region width along the  $OY$  axis is much more greater than the probing light beam diameter. The light beam radius in its waist equals  $a$  and it is placed at a distance  $L$  from the “input”. The screen (detector) is placed at distance  $z_D$  from the light beam “input”.

In this situation the dielectric constant of the medium in the thermally changed region is expressed by the equation

$$\epsilon(T) \equiv n^2(T) + 2n_0^2 s_T (T(\mathbf{r}) - T_0) = n_0^2 + \nu(\mathbf{r}). \tag{14}$$

The changes in probing beam are expressed by  $\nu$ .

In order to obtain disturbed probing beam parameters we apply the perturbation calculus [6]. The first correction to the eikonal can be expressed as

$$\psi(\tau) = \psi_0(\tau) + \psi_1(\tau) = \psi_0(\tau) + \frac{1}{2} \int_0^\tau \nu(\mathbf{r}_0(\tau')) d\tau', \tag{15}$$

with the integration being carried out along the undisturbed ray trajectory. It means that the amplitude of the Gaussian beam in the plane of detector has the form

$$A(\mathbf{r}_D) \equiv A_0(z_D). \tag{16}$$

Finally, the electric field distribution of probing beam on the surface of detector (quadrant photodiode) can be written as

$$u(\mathbf{r}_D) = A_0(\mathbf{r}_D) \exp[ik\psi(\mathbf{r}_D)] \tag{17}$$

where  $A_0$  is expressed by the first of Eqs. (10). Now, we are allowed to calculate the intensity distribution on that detector

$$I(\mathbf{r}_D) \propto |u(\mathbf{r}_D)|^2. \tag{18}$$

The concrete calculations depend on the form of dielectric constant disturbance Eq. (13) of the air, in which the probing beam propagates. This disturbance in our case is determined by temperature field. The form of temperature distribution in gas over the sample depends on many parameters of the experimental setup, which are defined by the proper boundary conditions. In this work, a model presented in [8] was used. For such assumptions the temperature distribution in the gas directly over the sample (*i.e.*, in the region  $x_D > 0$ ,  $-\infty < y_D < +\infty$ ,  $z_l < z < z_p$ ) has the shape (comp. [9])

$$\begin{aligned} T(x, z) - T_0 &= \vartheta(x) = \\ &= \left[ \vartheta + \theta_g \exp\left(-\sqrt{\frac{\Omega}{2\kappa_g}}(x+h)\right) \cos\left(\Omega t - \sqrt{\frac{\Omega}{2\kappa_g}}(x+h) + \gamma_g\right) \right] H[(z-z_l)(z_p-z)] \end{aligned} \quad (19)$$

where:  $\kappa_g$  – thermal diffusivity of gas,  $\vartheta_g$  – an increase of the gas temperature constant,  $\theta_g$  – amplitude of temperature changes on the surface of the sample,  $\gamma_g$  – phase shift between the sample surface temperature and the pumping beam,  $H(s)$  – Heaviside's step function. From expression (19) all fundamental properties of the thermal waves can be deduced; these are highly damped waves (the attenuation coefficient equals the wave number) and they also have strong dispersion. Although the sample stimulation is not strictly harmonic, at a sufficient distance from the sample surface in the thermal perturbation spectrum only its fundamental component is observed. The parameters  $\theta_g$  and  $\gamma_g$  depend on the angular modulation frequency  $\Omega$ , other experimental parameters also depend on thermal properties of the sample.

The eikonal change of the Gaussian beam on the basis of Eqs. (13) and (15) can be written as

$$\psi_1(\tau) = n_0^2 s_T \int_0^\tau \vartheta(x(\tau'), z(\tau')) d\tau' \quad (20)$$

where

$$\vartheta(x, z) = \left[ \vartheta_g + b_g \exp\left(-\sqrt{\frac{\Omega}{2\kappa_g}}x\right) \cos\left(\Omega t - \sqrt{\frac{\Omega}{2\kappa_g}}x + \varphi_g\right) \right] H[(z-z_l)(z_p-z)], \quad (21)$$

and

$$b_g = \theta_g \exp\left(-h \sqrt{\frac{\Omega}{2\kappa_g}}\right),$$

$$\varphi_g = \gamma_g - h \sqrt{\frac{\Omega}{2\kappa_g}}.$$

Integration in (20) is carried out along the undisturbed ray trajectory (Eqs. (11) and (12)). For simplification, the integration is done by middle point approximate methods.

Finally, we obtain

$$\psi_1(\tau) = [n_0^2 s_T \vartheta_g + \psi_{1f}] \tau_{pl} \tag{22}$$

where

$$\psi_{1f} = n_0^2 s_T b_g \exp(-k_g x_{0s}) \cos(\Omega t - k_g x_{0s} + \varphi_g) = \psi_{1fR} + i \psi_{1fI}, \tag{23}$$

$$x_{0s} = x(\tau_s) = x_D \frac{z_R + i(n_0 \tau_s - L)}{z_R + i(z_D - L)}, \tag{24}$$

$$\tau_s = \frac{1}{2} [(\tau + \tau_l)H(\tau - \tau_l) - (\tau - \tau_p)H(\tau - \tau_p)], \tag{25}$$

$$\tau_{pl} = (\tau - \tau_l)H(\tau - \tau_l) - (\tau - \tau_p)H(\tau - \tau_p). \tag{26}$$

In Equation (23), functions  $\psi_{1fR}$  and  $\psi_{1fI}$  are accordingly the real and complex parts of the correction to the eikonal. The phase of the wave can be written as

$$\psi(\mathbf{r}) \equiv \psi_0(\mathbf{r}) + \psi_1(\mathbf{r}) \tag{27}$$

where functions  $\psi_0$  and  $\psi_1$  are defined by Eqs. (10) and (22). In this case, the electric field distribution in the plane of detection of probing beam has the form

$$u(\mathbf{r}_D) \equiv A_0(z_D) \exp[ik(\psi_0(\mathbf{r}_D) + \psi_1(\mathbf{r}_D))], \tag{28}$$

and as a result the Gaussian beam intensity distribution can be written as

$$I(\mathbf{r}_D) \propto |u(\mathbf{r}_D)|^2 \equiv |A_0(z_D) \exp[ik\psi_0(\mathbf{r}_D)]|^2 \exp[-2k\psi_{1fI}(\mathbf{r}_D)\tau_{pl}]. \tag{29}$$

Taking into account that  $I_{0g}$  is the undisturbed Gaussian beam intensity distribution and  $|2k\psi_{1fI}\tau_{pl}| \ll 1$ , we finally obtain

$$I(\mathbf{r}_D) = I_{0g}(\mathbf{r}_D) - 2k\psi(\mathbf{r}_D)\tau_{pl}I_{0g}(\mathbf{r}_D) = I_{0g}(\mathbf{r}_D) + I_V(\mathbf{r}_D). \tag{30}$$

### 5. Normal signal from quadrant photodiode

The current signal from the photodiode under reverse bias is proportional to the intensity of light incident on it. In this the signal being case analyzed arises from the illumination difference between the upper and lower photodiode halves

$$S_{nk} = K_d \int_{-\infty}^{+\infty} dy_D \left( \int_0^{+\infty} - \int_0^{-h} \right) dx_D I(\mathbf{r}_D) \tag{31}$$

where  $K_d$  – photodetector constant (its sensitivity). In expression (31), it was regarded that the sample conceals a part of the photodiode (in the region  $-\infty < x_D < -h$ ). Proceedings as in [8], we obtain

$$S_{nk} = A_k \cos(\Omega t + \varphi_g - \varphi_k) \quad (32)$$

where

$$A_k = \frac{1}{2} \sqrt{\frac{\pi}{f}} K_d n_0^2 s_T b_g k I_m (z_p - z_l) \sqrt{(F_{1l} + F_{2l})^2 + (F_{2R} - F_{1R})^2}, \quad (33)$$

$$\tan \varphi_k = \frac{F_{2R} - F_{1R}}{-(F_{1l} + F_{2l})}, \quad (34)$$

$$F_1 = \exp\left(\frac{1+i}{2\sqrt{f}} C_x\right)^2 \left[1 - 2\operatorname{erf}\left(\frac{1+i}{2\sqrt{f}} C_x\right) + \operatorname{erf}\left(\frac{1+i}{2\sqrt{f}} C_x - h\sqrt{f}\right)\right] = F_{1R} + iF_{1i}, \quad (35)$$

$$F_2 = \exp\left(\frac{1-i}{2\sqrt{f}} C_x\right)^2 \left[1 - 2\operatorname{erf}\left(\frac{1-i}{2\sqrt{f}} C_x\right) + \operatorname{erf}\left(\frac{1-i}{2\sqrt{f}} C_x - h\sqrt{f}\right)\right] = F_{2R} + iF_{2i}, \quad (36)$$

$$C_x = k_g \frac{z_R + i(z_s - L)}{z_R + i(z_D - L)} = x_{0s} \frac{k_g}{x_D}, \quad z_s = n_0 \tau_s, \quad (37)$$

$$I_m = \frac{a_c P_l}{\sqrt{\pi} a \sqrt{a_c^2 + (L - z_D)^2}}, \quad f = \frac{a_c^2}{a^2 [a_c^2 + (L - z_D)^2]}. \quad (38)$$

In the last expression,  $P_l$  is the total power of undisturbed probing beam and  $\operatorname{erf}(\zeta)$  is the error function.

Waist coordinate of Gaussian beam  $L$  and its radius  $a$  in the waist depend on the focal length of the lens placed at the input of experimental setup. If  $a_0$  is the intensity radius of the beam incident on the lens and its waist is at the point of lens position ( $z = 0$ ), then  $a$  and  $L$  can be written in the form [10]

$$L = \frac{f}{1 + (f/z_l)^2}, \quad a = a_0 \frac{(f/z_l)}{\sqrt{1 + (f/z_l)^2}} \quad (39)$$

where  $f$  – focal length of the lens,  $z_l = (\pi a_0^2 n_0)/(4\lambda)$ .

The results of numerical calculations are presented by graphs with photothermal signal amplitude  $A_k$  [arb. u.] and additional phase shift  $\varphi_k$  [rad] (*i.e.*, relatively to the temperature phase on the sample surface) depending on some experimental setup parameters.

In typical photothermal measurements the amplitude  $A_k(h)$  and phase  $\varphi_k(h)$  of photothermal signal dependence on distance between probing beam axis and illuminated sample (Fig. 2) are investigated. After analysing these graphs it can be concluded that the course of the curves is strongly dependent on both the probing beam diameter and angular modulation frequency.

Figure 3 presents the amplitude and phase of photothermal signal dependence on probing beam diameter for different angular modulation frequencies and heights of

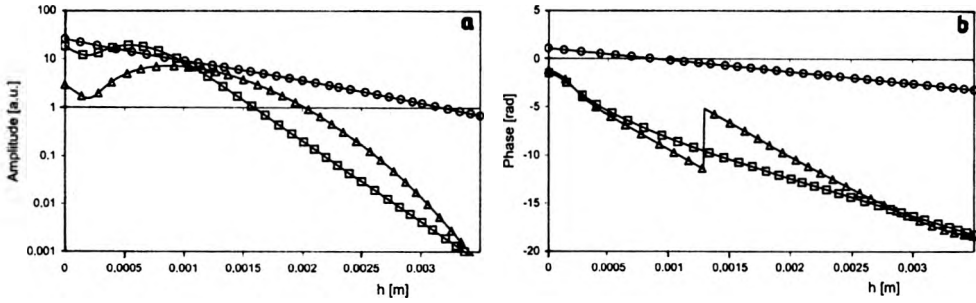


Fig. 2. Quadrant photodiode signal amplitude (a) and additional phase shift (b) changes vs. the probing beam height over the sample ( $z_D = 1.5$  m,  $z_p = 0.505$  m,  $z_l = 0.5$  m,  $L = 0.5$  m;  $-\square-$   $h = 200$   $\mu\text{m}$ ,  $\Omega = 60$  rad/s,  $-\triangle-$   $h = 200$   $\mu\text{m}$ ,  $\Omega = 600$  rad/s,  $-\circ-$   $h = 800$   $\mu\text{m}$ ,  $\Omega = 600$  rad/s).

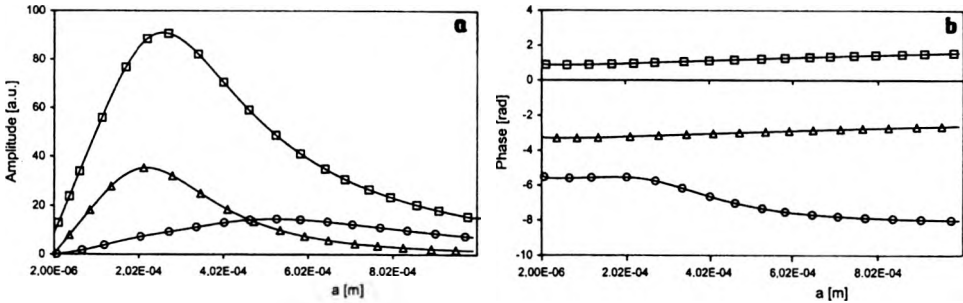


Fig. 3. Quadrant photodiode signal amplitude (a) and additional phase shift (b) changes vs. the probing beam diameter ( $z_D = 1.5$  m,  $z_p = 0.505$  m,  $z_l = 0.5$  m,  $L = 0.5$  m;  $-\square-$   $a = 500$   $\mu\text{m}$ ,  $\Omega = 600$  rad/s,  $-\triangle-$   $a = 1$  mm,  $\Omega = 600$  rad/s,  $-\circ-$   $a = 50$   $\mu\text{m}$ ,  $\Omega = 60$  rad/s).

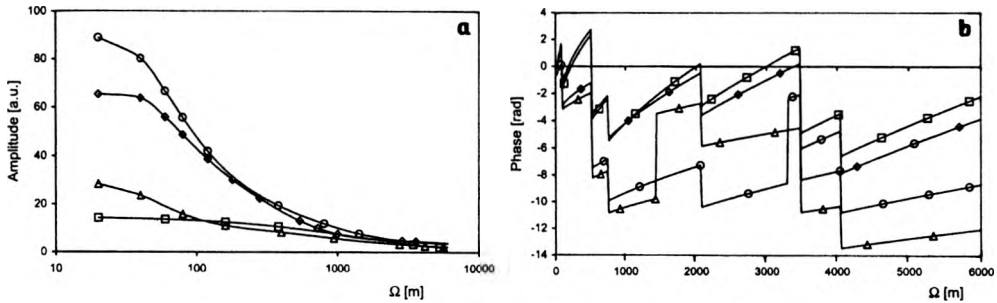


Fig. 4. Quadrant photodiode signal amplitude (a) and additional phase shift (b) changes vs. the modulation angular frequency ( $z_D = 1.5$  m,  $z_p = 0.505$  m,  $z_l = 0.5$  m,  $L = 0.5$  m;  $-\square-$   $a = 50$   $\mu\text{m}$ ,  $h = 200$   $\mu\text{m}$ ,  $-\diamond-$   $a = 500$   $\mu\text{m}$ ,  $h = 800$   $\mu\text{m}$ ,  $-\circ-$   $a = 500$   $\mu\text{m}$ ,  $h = 800$   $\mu\text{m}$ ,  $-\triangle-$   $a = 1$  mm,  $h = 800$   $\mu\text{m}$ ).

the probing beam over the sample. For a certain beam diameter the signal amplitude reaches a maximum value. This maximum shifts towards higher values of beam diameter when the height of the probing beam over the sample grows and it gets smaller when the angular modulation frequency increases.

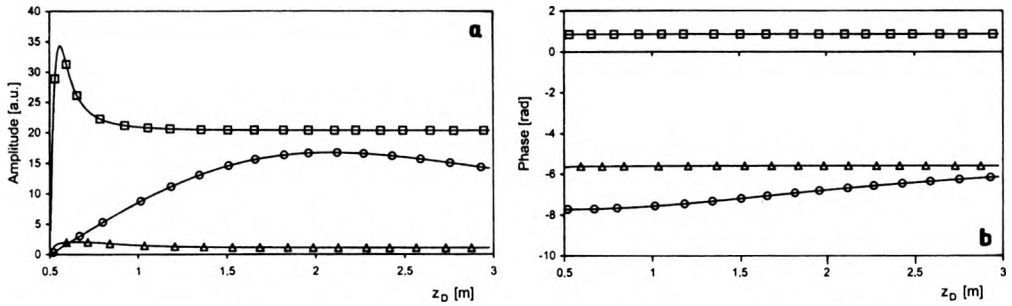


Fig. 5. Quadrant photodiode signal amplitude (a) and additional phase shift (b) changes vs. the detector position ( $z_p = 0.505$  m,  $z_l = 0.5$  m,  $L = 0.5$  m;  $-\square-$   $\Omega = 60$  rad/s,  $a = 50$   $\mu$ m,  $h = 200$   $\mu$ m,  $-\triangle-$   $\Omega = 600$  rad/s,  $a = 50$   $\mu$ m,  $h = 800$   $\mu$ m,  $-\circ-$   $\Omega = 600$  rad/s,  $a = 500$   $\mu$ m,  $h = 800$   $\mu$ m).

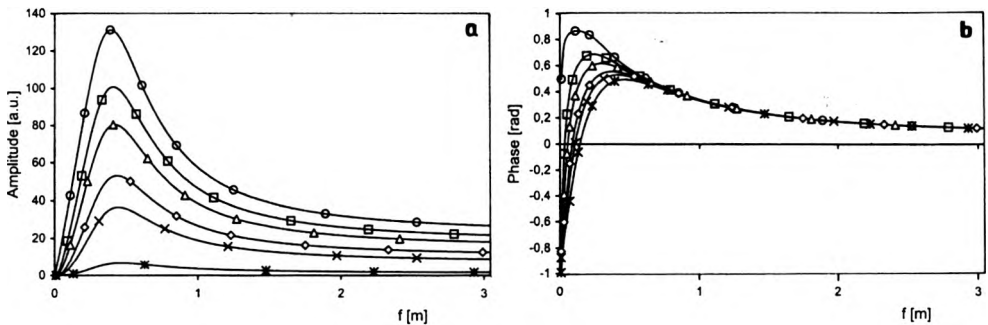


Fig. 6. Quadrant photodiode signal amplitude (a) and additional phase shift (b) changes vs. the focal length ( $z_D = 1.5$  m,  $L = 0.5$  m;  $-\circ-$   $z_p = 0.035$  m,  $z_l = 0.03$  m,  $-\square-$   $z_p = 0.305$  m,  $z_l = 0.3$  m,  $-\triangle-$   $z_p = 0.505$  m,  $z_l = 0.5$  m,  $-\diamond-$   $z_p = 0.805$  m,  $z_l = 0.8$  m,  $-\times-$   $z_p = 1.005$  m,  $z_l = 1$  m,  $-\ast-$   $z_p = 1.405$  m,  $z_l = 1.4$  m).

It can be seen from Fig. 4 that the signal from quadrant photodiode dramatically decreases with an increase of angular modulation frequency.

In Figure 5, the dependence of photothermal signal on detector coordinate for different angular modulation frequencies, different probing beam radii and its height over the sample is presented. There can also be seen a dramatic drop of the signal when the beam waist is over the detector and a dramatic rise when the beam waist is a bit in front of or behind it.

Figure 6 shows that the focal length influences the value and the shape of the photothermal signal. The lens was placed at the input of our experimental setup. The signal reaches a maximum and its position is independent of the sample position between the input and the detector. The value of the signal drops when approaching the detector.

Figure 7 shows the dependence of the signal amplitude and additional phase shift on the sample and waist position of probing beam. The sample and waist position was changed so that the beam waist was always over the sample. The value of the signal decreases while approaching the detector.

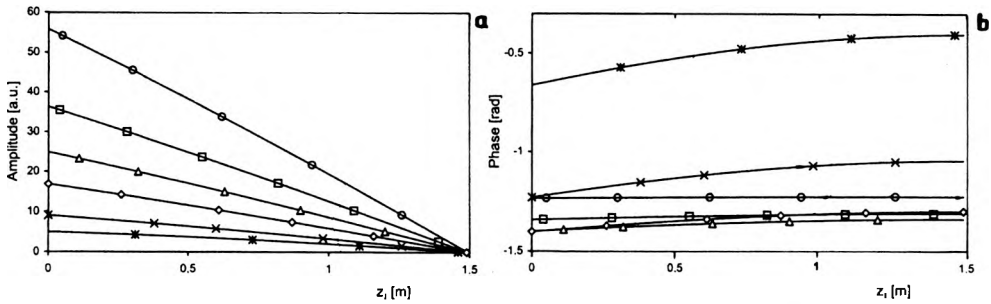


Fig. 7. Quadrant photodiode signal amplitude (a) and additional phase shift (b) changes vs. the sample position and beam waist position ( $z_D = 1.5$  m,  $h = 200$   $\mu$ m;  $-\circ-$   $\Omega = 60$  rad/s,  $-\square-$   $\Omega = 120$  rad/s,  $-\triangle-$   $\Omega = 200$  rad/s,  $-\diamond-$   $\Omega = 320$  rad/s,  $-\times-$   $\Omega = 600$  rad/s,  $-\ast-$   $\Omega = 1200$  rad/s).

Some discontinuities can be seen on the graphs with phase change of photothermal signal from quadrant photodiode. They result from only “partial” phase normalization of the signal to the range  $(0, 2\pi)$ .

## 6. Conclusions

The influence of the different parameters of experimental set-up on signal value in photothermal investigations with mirage effect was analysed in the work. The signal dependence on such parameters as probing beam radius, waist position, focus length of the input optical system, height over the sample surface and detector position was considered. A theory worked out on the basis of complex geometrical optics methods gives the possibility of taking into account many other parameters (*e.g.*, probing beam modulation frequency), which are important for interpreting the measurement results. One-dimensional thermal wave propagated in the gas over the sample excited by harmonically modulated pumping beam was taken into account. So-called phase normal signal created as a result of the phase change of the Gaussian beam probing this thermal wave was considered. Quadrant photodiode detection was analysed. The results are presented in analytical form and in the form of graphs and they can be used for experimental set-up optimisation.

## References

- [1] MURPHY J.C., AAMODT L.C., *J. Appl. Phys.* **51** (1980), 4580.
- [2] GLAZOV A., MURATIKOV K., *Opt. Commun.* **84** (1991), 283.
- [3] AAMODT L.C., MURPHY J.C., *J. Appl. Phys.* **52** (1981), 4903.
- [4] BUKOWSKI R.J., BODZENTA J., MAZUR J., KLESZCZEWSKI Z., *Parameter Estimation in Photothermal Measurements with Photodeflectional Detection*, [In] *Nondestructive Characterization of Materials VII, Part 1, Proceedings of the Seventh International Symposium on Nondestructive Characterization of Materials held in Prague, Czech Republic, June 1995*, pp. 295–302, Transtec Publications 1996.
- [5] KRAWCOW JU.A., ORLOV JU.I., *Geometrical Optics of the Nonhomogeneous Media* (in Polish), [Ed.] WNT, Warszawa 1993.

- [6] BUKOWSKI R.J., *Complex geometrical optics application for description of the Gaussian beam propagation in optically nonhomogeneous media*, [In] Proc. 2nd Nat. Conf. *Physical Basis of the Nondestructive Investigations*, Gliwice Chapter of the Polish Physical Society and Institute of Physics of the Silesian University of Technology, Gliwice 1997, pp. 45–55, (in Polish).
- [7] BUKOWSKI R.J., Proc. SPIE **3581** (1998), 285.
- [8] BUKOWSKI R.J., *Complex geometrical optics application for analysis of different methods detection in photothermal measurements* (in Polish), Zesz. Nauk. Pol. Śl., Seria: Matematyka–Fizyka, No. 87 (1999), pp. 37–54.
- [9] CARSLAW H.S., JAEGER J.C., *Conduction of Heat in Solids*, Oxford University Press, Oxford 1959.
- [10] YARIV A., YEH P., *Optical Waves in Crystals, Propagation and Control of Laser Radiation*, Wiley, New York 1984.

*Received March 12, 2002*